Petrographical characteristics as an indicator of physico-mechanical properties of concrete aggregate

Petrographical characteristics as an indicator of physico-mechanical properties of concrete aggregate

L Bianco[1,2*] **and G Micallef**[3]

[1] Faculty for the Built Environment, University of Malta
[2] Faculty of Architecture, University of Architecture, Civil Engineering and Geodesy, Sofia, Bulgaria
[3] CVC Architecture Studio, Valletta, Malta

* lino.bianco@um.edu.mt

Abstract. The physical and mechanical properties of concrete designed to a C40 mix using 6.5 mm and 10.0 mm aggregate from Montenegro and Malta respectively were investigated. Ultrasonic pulse velocity (UPV) and compressive strength (CS) tests corroborated findings in the literature. The coarseness of aggregate was found to be of primary technological importance: CS increased with increasing aggregate size. Although UPV in all the tests was between 3.5 km/s and 4.5 km/s – that is the concrete quality was of good grade – the CS of the control cubes for the 6.5mm and 10.0mm coarse aggregate mixtures was 27 N/mm^2 and 39 N/mm^2 respectively. The homogeneity of the concrete was affected by the physical and mechanical properties of the aggregate, including its size, but its petrological texture was also a significant parameter. The petrological characteristics of the aggregate severely affected the load-bearing capacity of the concrete. These characteristics had a significant bearing on the physico-mechanical properties of the hardened concrete.

1. Introduction

Concrete is a widely used construction material [1], a statement upheld by [2] in their recent study on the properties of multi-recycled concrete. Aggregate is the main ingredient which accounts for nearly 75% of the volume, with the coarser fraction, depending on the mix proportions, accounting for 50 to 60% of the mix.

Recent research addressed the process of designing a prototype coffee table, from drawing to the production of an industrial item [3]. The final product made extensive use of concrete, walnut-finished timber components and black-finished steel elements (figure 1). Concrete was utilised both in plane and edge orientations, the latter being useful to enhance the minimum thickness possible in order to reflect the concept of lightness. Whilst weight was a major drawback, concrete was nevertheless selected as the dominant product material. The surfaces were produced from freshly poured concrete in 25mm deep moulds designed for the panels. There were 5 moulds, each varying in form to correspond to the panels. They were constructed from melamine laminated particle board for (i) the production of a smooth finish and (ii) ease of demoulding. The sides of the moulds were manufactured in sanded pine wood as mitre edges could not be produced in melamine.

Figure 1. Coffee table: conceptual impression (a) and finished product (b).

The design strength for the required concrete was set between 35 MPa and 40 MPa and thus a C40 concrete mix design was utilised. Two mixtures were used, differentiated by the type and size of the coarse aggregate: 6.5 mm aggregate from Montenegro and 10 mm aggregate from Malta. Whilst the panels manufactured from the 10 mm aggregate were not damaged on demolding after the 7-day curing period (figure 2a), the 6.5 mm aggregate panels were damaged at the edges (figure 2b) and one failed at the corner (figure 2c). The aim of this paper is to investigate why these panels failed when, at face value, they had the most appropriate aggregate available on the market for the design mix. Given that all the basic components were uniform except for the type and size of aggregate, the study investigated their texture.

Figure 2. Concrete panels after a 7-day curing period using 10.0 mm (a) and 6.5 mm (b and c) aggregate.

2. Methodology

2.1. Materials

Portland limestone cement CEM II/A-LL 42.5 R and local potable tap water were used in all the mixtures. Silica fume was introduced to improve the strength of the concrete. The coarse aggregate was of two sizes: 6.5 mm and 10.0 mm. According to the aggregate supplier, the former was from Volujica Quarry in Port of Bar, Montenegro. The latter was from Wied Filep Quarry HM22 located at the limits of Naxxar, Malta. The aggregate from Montenegro fell within the 4 to 8 mm size range supplied by the company processing the limestone. The characteristics of the aggregate met the specifications of the European Directive for building materials and CPR 305/2011 standard EN 12620: 2002 + A1: 2008 (http://www.nimont.me/quarry.php). The fine aggregate used in all the mixes was

from the quarry in Malta. The Volujica Formation outcrops at Bar and is composed of Late Cretaceous sediments of banked and stratified limestone with dolomite interbeds. Light brown banks, thick bedded rudist bioclastic biomicrites, lumakeles, and konkins are intercalated with dark brown medium beds of wackestones [4, 5]. The formation which outcrops at Naxxar is the Oligocene Lower Coralline Limestone [6-8], specifically the Magħlaq Member which is the oldest limestone quarried and distinguished for its high crushing value [9].

2.2. Type and size of aggregate

Particle density and water absorption were determined as per [10] whilst the Aggregate Impact Value (AIV) was determined as per [11], now replaced by [12]. To study the texture at micro level, two samples of each type of aggregate were studied in thin section under a petrological microscope. The samples were selected through quartering.

2.3. Mix design and casting of concrete

The mix design for the C40 concrete is given in Table 1. Silica fume was added at 5% by weight of cement. To ensure consistency in the quality, quartering was used for both the fine and coarse aggregate. The mixture was produced by an electricity-driven concrete mixer and the water-cement ratio was kept at 0.55.

Two mixtures were cast: one for each size of the coarse aggregate. For a given mixture, the 5 moulds for the panels were cast at the Laboratory of Civil and Structural Engineering of the University of Malta. Following mixing for a duration of 15 minutes, the concrete was poured into each mould. The moulds were on a vibrating table to aid compaction, to limit entrapped air and to the fill the moulds to the edges. Trowelling was used to give an even finish to the panels. Four 100 x 100 x 100 mm concrete cubes were cast as a control unit.

The melamine-laminated moulds were thoroughly cleaned between each cast; no lubricant was utilised on their surface. Both the panels and cubes were cured for 7 days under plastic sheet covering until they were demoulded and left to air-cure for the remaining 28-day period.

Table 1. C40 mix design.

	Cement	Water	Aggregate [kg]		Silica fume
	[kg]	[l]	fine	coarse	[kg]
Per m^3 (to nearest 5 kg)	345	190	761	929	17.25
Per trial mix of 0.034 m^3	11.73	6.46	25.87	31.59	00.59

2.4. Testing regimes

A Zeiss Axioskop 40 transmitted light-microscope was used to analyse the thin sections of the coarse aggregate samples to establish the texture, porosity and permeability of the material:

- 6.5 mm aggregate: Sample I-1 and Sample I-2; and
- 10.0 mm aggregate: Sample C-1 and Sample C-2.

A ProgRes GT3 digital camera was used to capture images in both plane-polarized and cross-polarized light. The petrographical analysis and microphotographs were undertaken at the Department of Palaeontology, Stratigraphy and Sedimentology of the Geological Institute Strashimir Dimitrov, Bulgarian Academy of Sciences, Sofia.

To evaluate the physical-mechanical properties of the concrete cubes, two testing regimes were used on the 28th day:

- ultrasonic pulse velocity (UPV): in terms of [13], using the PUNDIT model and
- compressive strength (CS): in terms of [14], now superseded by [15], using Universal Testing Machine CONTROLS S.p.A. compression machine.

The cast panels were only subjected to the first of these regimes as it is a non-destructive test. Both tests were undertaken at the laboratory of the Department of Civil and Structural Engineering, Faculty for the Built Environment, University of Malta.

3. Results and discussion

3.1. Physical properties of aggregate

The particle density, water absorption and AIV for both aggregate sizes are given in Table 2. Although the 6.5 mm aggregate is marginally denser (3.8%) than the 10.00 mm aggregate, the latter is 21 times more water absorbent. The AIV of the larger-sized aggregate is 12.2% higher.

Table 2. Particle density, water absorption and Aggregate Impact Value of aggregates

	Coarse aggregate	
	6.5 mm	10.0 mm
Particle density – oven-dried (mg/m^3)	2.67	2.22
Particle density – saturated and surface dried (mg/m^3)	2.68	2.36
Apparent particle density (mg/m^3)	2.70	2.60
Water absorption (%)	0.30	6.30
AIV (%)	23.70	26.60

3.2. Petrographical characteristics of aggregate

Both Samples I-1 and I-2 are completely recrystallized limestone consisting of sparry calcite mosaics (figure 3a-f). The sizes of the calcite crystals in the former vary from 0.10×0.10 to 3.0×1.5 mm whilst in the later they vary from 0.10×0.10 to 1.5×0.5 mm. With respect to Sample I-1, the limestone was most probably originally composed of fossils and/or bioclasts, which are of aragonite and high-Mg calcite composition. The aragonite and high-Mg calcite are unstable polymorphs and easily recrystallize into stable low-Mg calcite during diagenesis. The recrystallization completely obliterates the original limestone texture. Single and poorly expressed stylolites can be observed (figure 3b). These were formed as a result of a pressure-dissolution process arising from overburden sedimentation or tectonic pressure. The stylolites are outlined by the presence of a dark brown to black insoluble residue that contains single, very fine-sized quartz grains (figure 3b). In Sample I-2, dispersed black organic matter is observed in the mosaics. Several terrigenous quartz grains are recognized (with a maximum size of 0.3×0.2 mm) (figure 3c and figure 3d), as well as rare well-formed crystals of diagenetic quartz. Single dissolution seams (figure 3e and figure 3f) and stylolites can be observed (figure 3f). These are also impregnated (lined) with a dark brown to black insoluble residue containing sporadic very fine-sized quartz grains (figure 3f).

Samples C-1 and C-2 are micrite limestones with fine bioclasts. According to Dunham's textural classification [16] they represent fine bioclastic wackestones because the matrix to allochems ratio is 80:20 and 85:15 for Sample C-1 and Sample C-2, respectively. In Sample C-1 micrite crystals (sizes < 4 μm) that construct micrite matrix are irregularly recrystallized to form microspar (min. ≥ 4 μm; max. ≤ 10 μm) and rarely to spar (> 10 μm) (Figure 4a). Fine bioclasts are the main allochems. Their sizes are ≤ 0.5 mm. Most bioclasts are completely recrystallized (figure 4a, RB) and some are highly altered and difficult to recognize (figure 4b, RB). Occasionally, preserved fragments of echinoids (with maximum size 0.4×0.2 mm), bryozoa (Figure 4c, BR) and bivalve shells (figure 4c, BSH) are present. Single benthic foraminifera occur (figure 4a, F). Some fragments resemble algae (figure 4a, A). In places in the matrix, peloids < 0.15 mm in size (figure 4b, MP), which are composed of dark micrite, are present. There are single quartz grains (figure 4a, Q) which are silt sized (< 0.063 mm).

In Sample C-2, the micrite in the matrix is often recrystallized into microspar and spar (figure 4d). Fine bioclasts (with sizes predominantly < 0.5 mm) are the main allochems (figure 4e, RB). Most often they are recrystallized and/or altered and are difficult to determine. One more preserved fragment of bivalve shell (1.5×0.01 mm in size) (figure 4e, BSH) can be seen. Some bryozoa bioclasts (up to a maximum length of 1.5 mm) are found. Benthic foraminifera are sporadically represented (figure 4d, F). Interparticle porosity, mainly observed in the matrix, is about 5% (figure 4d).

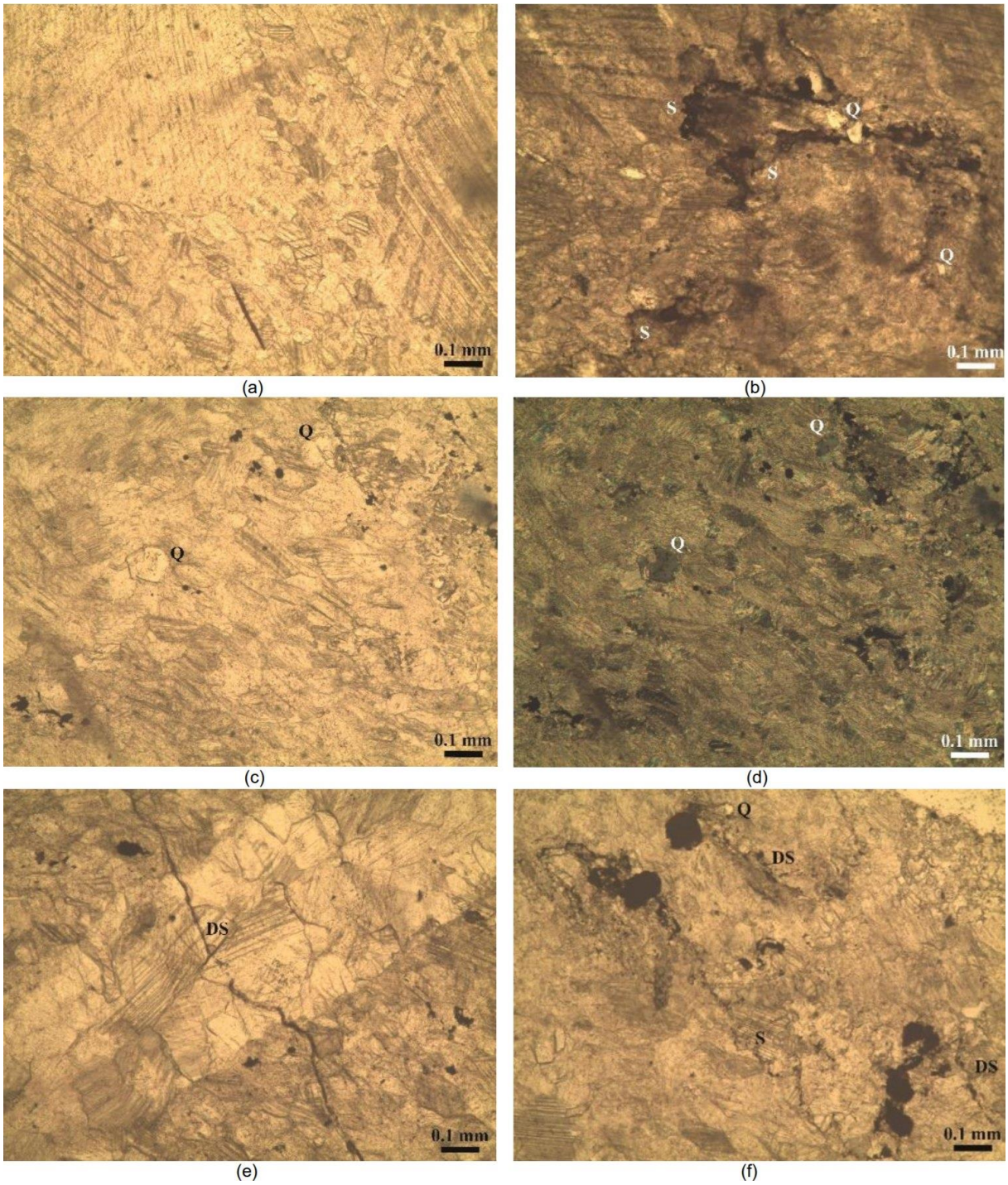

Figure 3. *Sample I-1:* plane-polarized light: (a) sparry calcite mosaics, calcite crystals are of various sizes and (b) plane-polarized light: sparry calcite mosaics with poorly expressed stylolites (S) and single quartz grains (Q); *Sample I-2:* (c) plane-polarized light: sparry calcite mosaics, calcite crystals are of various sizes and single quartz grains (Q), (d) cross-polarized light: same view as (c), (e) plane-polarized light: sparry calcite mosaics crossed by dissolution seam (DS) and (f) plane-polarized light: sparry calcite mosaics with poorly expressed stylolites (S), dissolution seams (DS) and single quartz grains (Q).

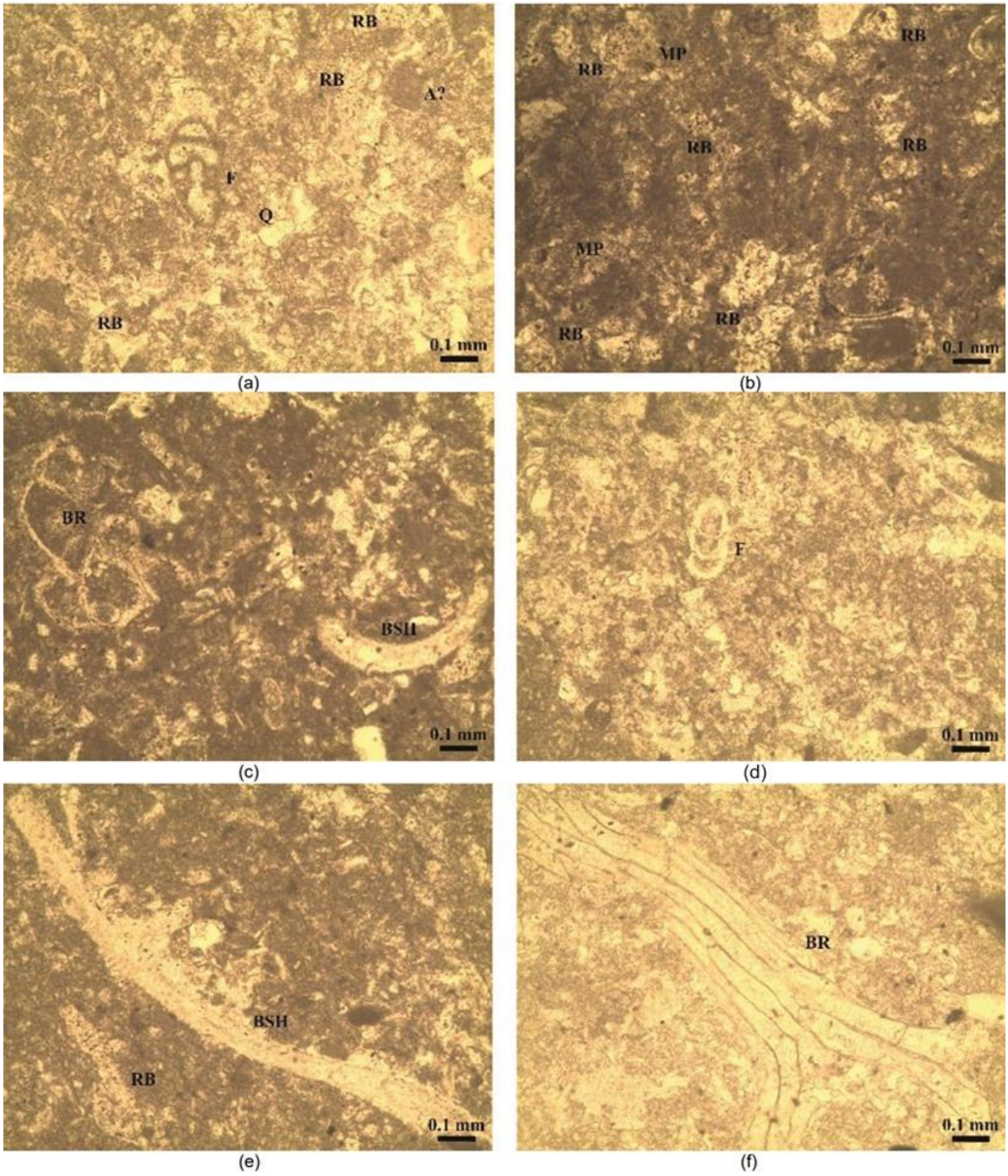

Figure 4. *Sample C-1:* plane-polarized light: (a) micrite matrix is irregularly recrystallized to microspar and spar, recrystallized bioclasts (RB), alga fragment (A?), foraminifera (F) and quartz grain (Q), (b) completely recrystallized and highly altered bioclasts (RB) and micrite peloids (MP) and (c) fragments of bryozoa (BR) and bivalve shell (BSH); *Sample C-2:* plane-polarized light: (c) micrite matrix is irregularly recrystallized to microspar and spar, foraminifera (F), (e) recrystallized bioclasts (RB) with part of more preserved fragment of bivalve shell (BSH) and (f) a part of more preserved fragment of bryozoa (BR).

3.3. UPV and CS

Figure 5 illustrates the effect of varying coarse aggregate size on the UPV and CS after a 28-day curing process. The UPV for the cast panels is given in Table 3. The UPV and the CS of the control cubes are given in table 4. The UPV for concrete manufactured with 6.5 mm and 10.0 mm aggregate is plotted for the panels in figure 5a and for the cubes in figure 5b; the CS for the cubes is plotted in figure 5c. Strong correlations exist between UPV and CS for rocks and concrete; UPV increases with the increase in CS [17]. Regression analysis shows a reliable correlation of UPV with compressive strength for high porous limestone in dry and wet conditions, both lowered in the later conditions [18]. Given that the UPV for both the panels and the cubes is between 3.5km/s and 4.5km/s, the concrete quality is of good grade in terms of uniformity and homogeneity. There were no significant variations between the two aggregates [19].

Table 3. UPV of the concrete panels at 28th day

		Length l_1	Breath l_2	Height	Weight	Time* [ms]		UPV [km/s]	
		[mm]	[mm]	[mm]	[g]	t_1 across l_1	t_2 across l_2	V_1	V_2
6.5mm aggregate	Panel 1	392.00	502.00	25.93	10351.50	103.3		3.795	0.000
	Panel 2	392.00	504.00	25.27	09540.00	103.9		3.773	0.000
	Panel 3	391.00	502.00	26.55	10565.50		136.7	0.000	3.672
	Panel 4	334.00	501.00	26.14	09041.00		138.8	0.000	3.610
	Panel 5	104.00	503.00	25.09	02613.00	26.3		3.954	0.000
	Mean							3.841	3.641
10.0mm aggregate	Panel 1	390.00	504.00	24.19	8900.50	105.0		3.714	0.000
	Panel 2	390.00	502.00	24.88	9509.00	104.1		3.746	0.000
	Panel 3	391.00	500.00	24.77	9102.00		130.5	0.000	3.831
	Panel 4	335.00	504.00	24.00	7486.00		133.0	0.000	3.789
	Panel 5	103.00	503.00	24.60	2500.50	25.1		4.104	0.000
	Mean							3.855	3.810

* Measured along the parallel non-bevelled sides.

Table 4. UPV and CS of the concrete cubes at 28th day.

		l_1	l_2	Height	Weight	Time [ms]		UPV [km/s]		Loading*	Area	CS*
		[mm]	[mm]	[mm]	[g]	t_1 across l_1	t_2 across l_2	V_1	V_2	[kN]	[mm^2]	[N/mm^2]
6.5mm aggregate	Cube 1	100.48	100.32	95.49	2055.00	24.6	25.0	4.085	4.013	272.5	10080	27.03
	Cube 2	100.42	100.47	99.17	2098.50	24.8	25.1	4.049	4.003	260.5	10089	25.82
	Cube 3	100.47	100.51	99.30	2099.50	25.0	25.1	4.019	4.004	264.2	10098	26.16
	Cube 4	100.45	100.48	95.91	2043.50	24.9	25.0	4.034	4.019	276.7	10093	27.41
	Mean							4.047	4.010			26.61
10.0mm aggregate	Cube 1	100.38	100.40	100.98	2088.50	24.3	24.8	4.131	4.048	390.5	10078	38.75
	Cube 2	100.35	100.77	103.69	2092.50	25.0	24.2	4.014	4.164	400.3	10112	39.59
	Cube 3	100.63	100.68	101.19	2086.00	24.8	24.4	4.058	4.126	402.4	10131	39.72
	Cube 4	100.84	100.32	100.19	2054.50	24.9	24.6	4.050	4.078	396.6	10116	39.20
	Mean							4.063	4.104			39.31

* At crushing.

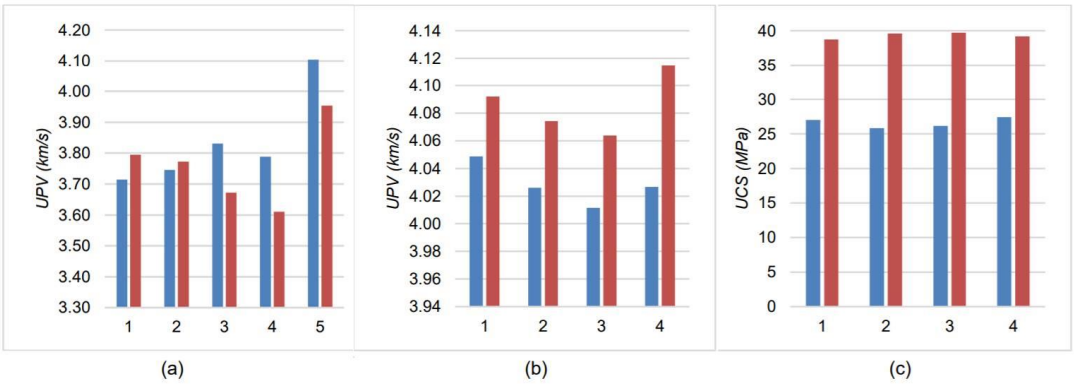

Figure 5. UPV after 28 days (air-cured) for panels (a) and for control cubes (b); CS after 28 days (air-cured) for control cubes (c). Blue and red refer to 6.5mm and 10.0mm aggregate respectively.

In the case of the 6.5 mm aggregate, the resultant mean CS of the concrete was 27 MPa, just above two-thirds the grade of the mix design; the resultant mean CS of the concrete using 10.0 mm aggregate was 39 MPa, close to the grade of the mix design. All cubes typically had a bell-shaped profile on crushing except for cubes 1 and 2 constructed in 6.5 mm aggregate, which exhibited shear failure [figure 6). Grade C40 is structural concrete. The strength of the concrete is dependent on its coarse aggregate. The homogeneity of the concrete decreases as the aggregate size increases [20]. Coarseness of aggregate is a parameter of primary technological importance. Although the UPV results met the standard of concrete quality, the concrete manufactured using the less coarse aggregate had significantly lower strength than that produced with the coarser aggregate.

Both aggregate types are supplied on the building construction market as having similar physico-mechanical properties. However, they are petrologically different and this directly affects the resulting compressive strength of the hardened concrete. For the same mix design, the 6.5 mm aggregate is derived from recrystallized limestone whose original texture has been obliterated, resulting in an almost impervious rock. This produces a significantly weaker concrete grade than the 10 mm aggregate from micrite limestone with fine bioclasts, whose micrite matrix has been recrystallised into microspar and spar.

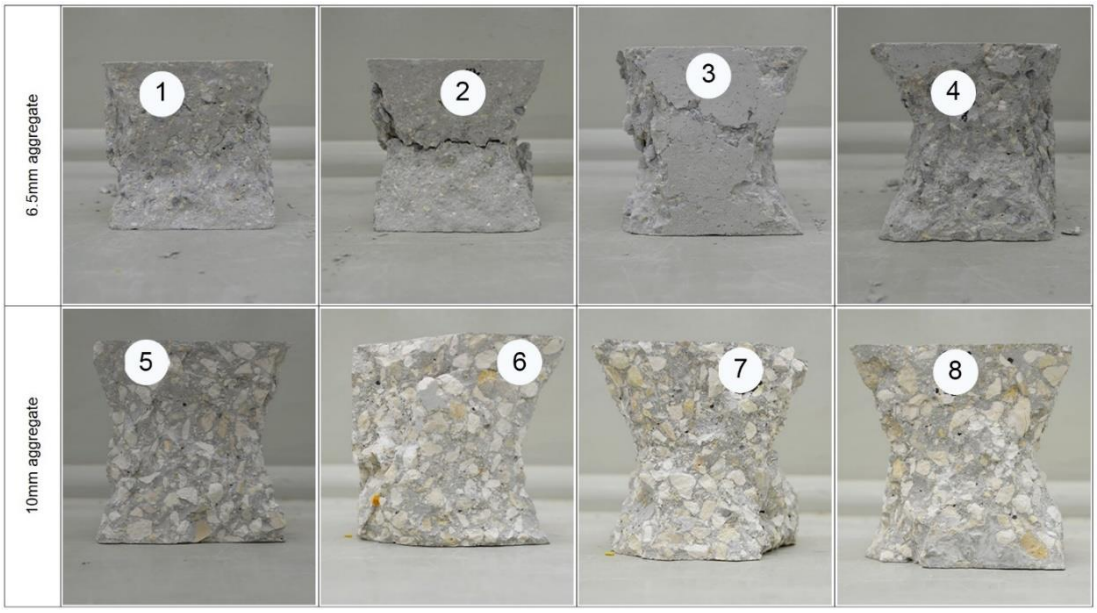

Figure 6. Uniaxial compressive test at 28 days: All cubes had a typically bell-shaped profile on crushing except for cubes 1 and 2, constructed in 6.5 mm aggregate, which exhibited shear failure.

4. Conclusions

Petrological characteristics are essential elements in aggregates because they have a significant bearing on the physico-mechanical properties of the hardened concrete. This study, which investigated the failure of concrete panels cast during the course of the manufacture of a prototype coffee table, confirmed that compressive strength increased with coarse aggregate size:

- For a C40 mix design, the grade of concrete attained by the 6.5 mm and 10.0 mm coarse aggregate, from limestones quarried from different lithostratigraphic formations, was 27 MPa and 39 MPa respectively. The 10.0 mm aggregate met the desired ultimate strength requirement but the 6.5mm aggregate reached just two-thirds of the mark.
- The apparent particle density of the 6.5 mm aggregate is higher than that of the 10.0 mm aggregate. In addition, it has lower AIV and significantly lower water absorption.
- The UPV test did not provide important data on the nature of the rock and the CS. Variation in the petrological and textural content of the rocks impacted the CS.

These findings have a broader impact. Although the size of the aggregate has a bearing on the CS of concrete, its petrological characteristics are indicative of its behaviour in the hardened concrete. The homogeneity of the concrete is affected by the physico-mechanical properties of the aggregate, including particle size, but its petrological texture significantly affects the load-bearing capacity of the hardened concrete. Thus, specifications of aggregate for concrete manufacture, which are normally stated in terms of physico-mechanical properties, should specifically include the geological provenance of the raw material used, as petrological properties vary between limestones from differing geological formations and origins.

5. Limitations

The study by [3] was undertaken to explore the shift from design to production phases in lieu of finding a better mode of communication between product design and manufacture, in this case using a prototype of a coffee table manufactured partly in concrete; it was not a study on concrete technology. The objective was to produce a mixture using 6.5 mm aggregate from Montenegro. After obtaining CS values well below the mix design the mixture was repeated using a 10.0mm aggregate from Malta, this being a limited sample from the last batch available at the Civil and Structural Engineering Laboratory of the University of Malta. The findings would have been expedient if the mixtures in both aggregate sizes were undertaken in material resulting from both sources.

Acknowledgements

The authors would also like to thank Professor Elena Koleva-Rekalova from the Geological Institute of the Bulgarian Academy of Sciences, Sofia, for the microphotographs and her advice on petrographical interpretations, and Nicholas Azzopardi, concrete technologist and senior laboratory officer at the Civil and Structural Engineering Laboratory, University of Malta, for his support in undertaking the physical testing of the materials focused on in this study.

The authors would like to acknowledge their gratitude to Martin Djakovic and Mileva Milić from the Geological Survey of Montenegro for professional support in describing the geology and petrography of the Volujica formation respectively.

References

[1] Nagaratnam S, Carthigesu T, Rabin T and Bobby K 2017 *Civil Engineering Materials* (Queensland, Australia: Cengage Leraning US).
[2] Azzaz R A, Chemrouk M and Ammar-Boudjelal A 2020 Rheological, physico-mechanical and durability properties of multi-recycled concrete *Advances in Concrete Construction* **9** 1 9-22.
[3] Micallef G 2018 *An Architecture of Communication: Exploring the gap between design and production* [University of Malta: M Arch dissertation).
[4] Cadjenovic D, Radulovic N, Milutin J. Ostojic Z, Cepic M and Dakovic M (2002-2013) *Geological Map of Montenegro: Podgorica-Sheet 3* (Podgorica Montenegro Geological

Survey of Montenegro).
[5] Cadjenovic D T 2020 *Terain's geological composition* (https://www.academia.edu/31543907/TERAINS _GEOLOGICAL_COMPOSITIONOURCES, retrieved on 08 March 2020)
[6] Oil Exploration Directorate 1993 *Geological map of the Maltese Islands: Shhet 1:Malta* (Malta: Oil Exploration Directorate, Office of the Prime Minister).
[7] Pedley H M, House M R and Waugh B 1976 The geology of Malta and Gozo. *Proceedings of the Geologists' Association* **87** (3) 325–341.
[8] Pedley H M 1978 *A new lithostratigraphical and palaeoenvironmental interpretation for the coralline limestone formations (Miocene) of the Maltese Islands* (London: H M S O).
[9] Bianco L 1995 The industrial minerals of the Maltese Islands *Hyphen* **7** *3) 111–118.
[10] BS EN 1097-6:2013 *Tests for mechanical and physical properties of aggregates. Determination of particle density and water absorption*.
[11] BS 812-111:1990 *Testing aggregates. Methods for determination of ten per cent fines value*.
[12] BS EN 1097-2:2010 *Tests for mechanical and physical properties of aggregates. Methods for the determination of resistance to fragmentation*.
[13] BS EN 12504-4:2004 *Testing concrete, Part 4: Determination of ultrasonic pulse velocity*.
[14] BS EN 12390-3:2009 *Testing hardened concrete. Compressive strength of test specimens*.
[15] BS EN 12390-3:2019 *Testing hardened concrete. Compressive strength of test specimens*.
[16] Dunham R J 1962 Classification of carbonate rocks according to depositional texture *Classification of carbonate rocks* ed W E Ham (Tulsa, Oklahoma: American Association of Petroleum Geologists) Memoir 1, pp 108-121.
[17] Sertçelik I, Kurtuluş C, Sertçelik F, Pekşen E and Aşçı M 2018 Investigation into relations between physical and electrical properties of rocks and concretes *Journal of Geophysics and Engineering* **15** 142.
[18] Vasanelli E, Colangiuli D, Calia A, Sileo M and Aiello M A 2015 Ultrasonic pulse velocity for the evaluation of physical and mechanical properties of a highly porous building limestone *Ultrasonic*s **60** 33-40.
[19] IS 13311 1992 Part I *Standard Code of Practice for Non-Destructive Testing of Concrete: Part 1 - Ultrasonic Pulse Velocity* (New Delhi: Bureau of Indian Standards).
[20] Tsiskreli G D and Dzhavakhidze A N 1970 The effect of aggregate size on strength and deformation of concrete *Hydrotechnical Construction* **4** 448-453.